

Correlation reflectometry in fusion plasmas—an application at TEXTOR

To cite this article: A Krämer-Flecken *et al* 2011 *Plasma Phys. Control. Fusion* **53** 074020

View the [article online](#) for updates and enhancements.

You may also like

- [Sustainability, collapse and oscillations in a simple World-Earth model](#)
Jan Nitzbon, Jobst Heitzig and Ulrich Parlitz
- [Transitions to new climates \(TNCs\) in the 21st century](#)
Filippo Giorgi and Francesca Raffaele
- [Quantifying human contributions to past and future ocean warming and thermohaline sea level rise](#)
Katarzyna B Tokarska, Gabriele C Hegerl, Andrew P Schurer et al.

Correlation reflectometry in fusion plasmas—an application at TEXTOR

A Krämer-Flecken¹, S Soldatov², Y Xu³ and T Zhang¹

¹ Institut für Energie- und Klimaforschung/Plasmaphysik, Forschungszentrum Jülich, Association EURATOM-FZJ, Germany

² Department of Applied Physics, Ghent University, Rozier 44, 9000 Gent Belgium

³ Ecole Royale Militaire/Koninklijke Militaire School, Euratom-Belgian State Association, Avenue de la Renaissance 30, B-1000 Brussels, Belgium

E-mail: a.kraemer-flecken@fz-juelich.de

Received 5 November 2010, in final form 9 March 2011

Published 18 May 2011

Online at stacks.iop.org/PPCF/53/074020

Abstract

Correlation reflectometry (CR) is based on the simultaneous measurement of two or more spatially separated antennae at one or more frequencies with a high spatial and temporal resolution. It is sensitive to plasma density fluctuations at a reflection layer deduced from reflections of a probing wave with a frequency in the mm range. In fusion plasmas it is an appropriate tool to investigate instabilities based on small scale structures or wave phenomena. Furthermore, it provides the measurement of plasma rotation perpendicular to the local magnetic field under the assumption of frozen turbulence.

An overview of CR diagnostics installed at different devices is presented. The different applications principles as measurement of turbulence properties e.g. decorrelation time and correlation length are highlighted. Also the measurement of the pitch angle to deduce the local magnetic field is discussed. Furthermore, the often used application to determine the turbulence rotation is presented.

Recent measurements at TEXTOR with two reflectometers and three distributed antennae arrays will be presented. The long range correlations of density and velocity oscillations of the geodesic acoustic mode are investigated. But also properties of the ambient turbulence are studied. Measurements of radial correlation length of the ambient turbulence are performed for two poloidal positions, too. From these measurements the scaling of the radial turbulence correlation length is found to be gyro-Bohm-like.

(Some figures in this article are in colour only in the electronic version)

1. Introduction

This paper is not meant as a tutorial on reflectometry. General information on this subject can be found in e.g. [1]. Also the various aspects of interpretation of density fluctuations in

comparison with 2D simulations are not covered. For this topic the reader is referred to [2] and references therein. Furthermore, the use of reflectometry in determination of the density profiles is not discussed. This paper focuses on the different aspects of correlation reflectometry (CR) and some selected results from recent experiments at TEXTOR.

One of the main scientific reasons to work with CR is the unsolved problem of the anomalous transport in fusion plasmas. Meanwhile scientists are convinced that small scale structures are responsible for the anomalous transport. The interaction between turbulence, radial electric field, rotation and its shear seems to be the major player in the understanding of the generation and sustainment of flows which can result in a transport barrier. A deeper understanding could result in tools for the generation of regions with reduced transport. Recent experiments at ASDEX Upgrade have shown that geodesic acoustic mode (GAM), a side band of zonal flows (ZFs) can contribute to the generation of transport barriers.

Looking at the underlying properties of drift waves which predict frequencies in the range $40 \leq f \leq 500$ kHz and wavelength in the order of several millimeters up to a centimeter, CR with its good spatial and temporal resolution is an appropriate diagnostic for those investigations. It is suitable for the investigation of low k wave number, long living structures in fusion plasmas. Having more than one antennae, aiming at the same flux surface, aligned in the poloidal direction and close to each other, measurements of turbulence decorrelation time (τ_{dc}) and turbulence correlation length (L_c) can be obtained. With three antennae spaced toroidally and poloidally the tilt angle of the turbulent structures can be measured. With antennae at sufficiently large spatial separation, long range correlation (LRC) properties can be investigated which allow us to study the three-dimensional structure of fluctuations and flows in the plasma. In addition to the estimation of turbulence properties it can be used to measure the turbulence rotation perpendicular to the magnetic field (B_\perp). From strongly rotating fluids it is known that small scale structures are rotating at the same speed as the fluid [3]. Experiments at ASDEX [4] and TEXTOR [5] have shown that the turbulence moves almost with the plasma rotation. Therefore, an additional phase velocity of the turbulence can be neglected as long as the plasma rotation is dominating.

The paper is organized as follows. After a short overview on analysis tools in section 2 an overview of installed CR diagnostics and its applications is given in section 3. In section 4 the experimental set up at TEXTOR with its different correlation measurements is presented. Section 5 will show some exemplary results obtained at TEXTOR, followed by a brief summary.

2. Analysis tools

The strength of CR is based on the fact that a time delay between two time series at two different spatial positions or two different probing frequencies will enhance repeating (correlated) turbulent structures and suppress uncorrelated noise. Even correlated oscillations with a small amplitude (below the noise level of a single time series) become visible with this technique. The cross correlation between two discrete time series X and Y from e.g. two receiving antennae is defined as

$$(X \star Y)[n] = \sum_{m=-\infty}^{\infty} X^*[m]Y[n+m], \quad (1)$$

where n, m are indices of the time series. Calculating the normalized cross correlation for different time lags (corresponding to different m) between the two time series results in figure 1. It allows us to estimate the delay time (Δt) for the two time series from two antennae spots separated by the distance s and denotes the time needed for the turbulent structure to propagate the distance s on the flux surface which is determined by the cutoff

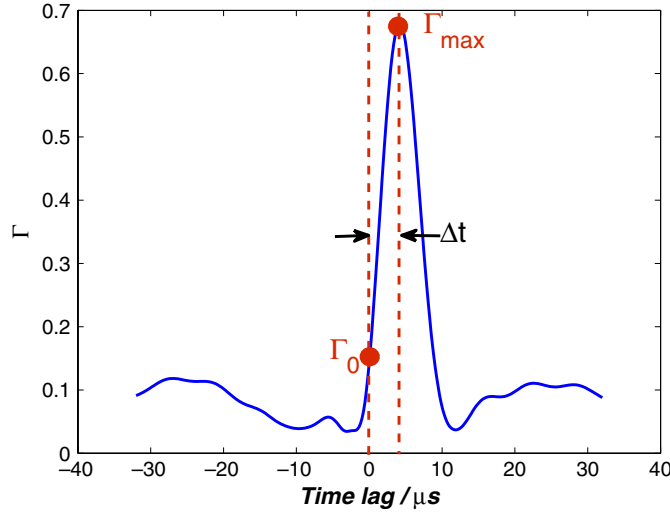


Figure 1. An example for the cross-correlation technique and the three determined quantities Δt , Γ_{\max} and Γ_0 .

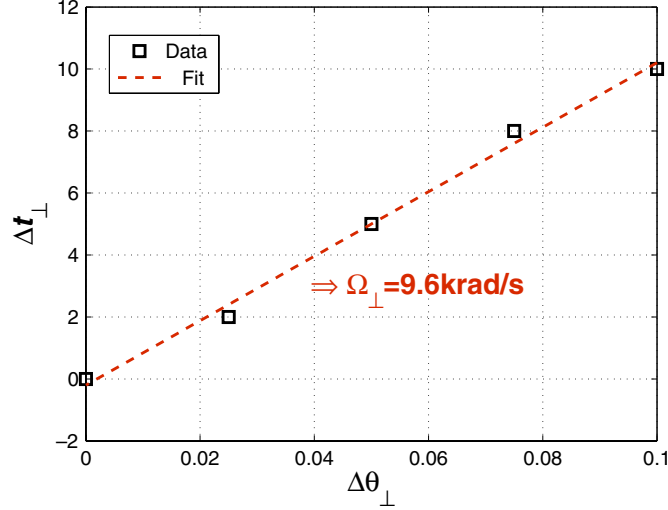


Figure 2. Determination of Ω_{\perp} from the slope of five different poloidal angles.

conditions of the probing wave. From $s/\Delta t$ the propagation speed of the structure in the plasma is calculated. Furthermore, the maximum cross-correlation coefficient $\Gamma(\Delta t)$ as well as the $\Gamma_0 = \Gamma(\Delta t = 0)$ can be measured. These quantities yield information on τ_{dc} and the correlation length (L_c). The propagation can be determined only if the following condition holds: $\tau_{dc} \geq \Delta t$.

Having several antennae all aligned, say along the poloidal direction, the slope of $\Delta t(\Delta\theta)$ gives the turbulence rotation, Ω_{\perp} , (see figure 2). The rotation is called in the perpendicular direction with respect to the field line along which the turbulence is aligned. The same analysis can be done for $\Gamma_{\max}(\Delta\theta)$. The measured values can be approached by a Gaussian shape. The full width at $1/e$ -level determines τ_{dc} of the turbulence. A similar procedure for $\Gamma_0(\Delta\theta)$ yields L_{\perp} , the perpendicular correlation length.

3. Correlation reflectometry

This section gives an overview on applications of CR diagnostics at different devices. In addition to the measurement of turbulence properties, the homodyne CR system at FT2 [6] is used to determine the mode number m, n of low-frequency MHD modes with two arrays of three antennae each. Each array spans an angle of $\Delta\theta = 0.16$ rad. The two arrays are separated by $\Delta\phi = \pi$ rad. From the observation of low-frequency oscillations and the cross correlation the poloidal and toroidal mode number is determined, and the safety factor q at the reflection layer r_c respectively. To estimate the local magnetic field CR at LAPD [7] is used as well. In this set up two reflectometers operating in the same frequency range are used. Scanning the X-mode reflectometer and keeping the O-mode at fixed frequency, the maximum in the cross correlation indicates that both systems probe the same reflection layer. Since the X-mode cutoff depends on the local magnetic field and the plasma frequency which is equal to the O-mode cutoff frequency, it is possible to determine the local magnetic field. This method is not followed up, mainly due to the fast decrease in the cross correlation with increasing B .

Another type of experiment has been performed at FTU [8] and T-10 [9]. In this device antennae arrays are used to measure turbulence spectral and correlation properties and rotation. At FTU a heterodyne system with two antennae arrays above and below the midplane are in operation. The upper array with four antennae for O-mode polarization and the lower array with two antennae for X-mode polarization. At X-mode the core plasma region becomes accessible up to $n_e = 2.9 \times 10^{20} \text{ m}^{-3}$. Mainly turbulence rotation measurements are performed and compared with MHD rotation. At T-10 three arrays are operated in one cross section at $\theta = 61^\circ$, $\theta = 116^\circ$ and $\theta = 180^\circ$ with respect to the outer midplane. Furthermore a 4th array has been recently installed at $\theta = 0^\circ$ and toroidally separated by 90° with respect to the other three arrays. The T-10 team investigated the turbulence propagation and found good agreement between plasma rotation and turbulence rotation [10]. This supports the theory that the plasma turbulence is mostly frozen in the plasma and obeys the same rotation as the plasma itself. In addition, first measurement on LRCs with CR are reported from T-10, by tailoring a discharge in a way that both antennae arrays are connected via a magnetic field line. Even if the coherence is small, it is significant and above the noise level.

At JET radial correlations are measured with a heterodyne system (X-mode) consisting of four fixed frequency reflectometers, each with two channels (with a spacing of $\Delta f \approx 10$ GHz). The 2nd channel scans in a small frequency range around the fixed frequency channel [11, 12]. The system is installed at the outer midplane. Radial correlations are measured in the pedestal region of the H-mode and a reduction in L_r , due to an increase in the rotation and shear, is found [13].

In addition to the conventional operating reflectometers, where the normal vector of the reflection layer and the incident wave vector are nearly parallel, Doppler reflectometry [14] has become an alternative, with an increasing number of installed systems. The main difference, the observation at a tilted angle between normal vector of r_c and the incident wave allows us to determine Ω_\perp from the Doppler shift in the spectrum of the reflected wave. The tilt angle (θ) determines the observed wave number range by the Bragg condition, $k_\perp = 2k_0 \sin \theta$, where k_0 denotes the wave number of the incident wave. By adjusting θ , k_\perp can be selected. Regarding hardware installation a clear advantage stems from the reduced antennae set up compared with normal CR. Operating several Doppler reflectometers allows us to make use of the same cross-correlation technique. Devices with much experience in Doppler reflectometry are AUG [4, 15] and Tore Supra [16]. Whereas in AUG all three Doppler reflectometers are installed in the same poloidal cross section below and above the midplane, a vertical Doppler system in addition to the one in the midplane is installed at Tore Supra. This system could give

information on LRCs if combined with the one of the two systems installed in the equatorial plane.

4. CR at TEXTOR

TEXTOR is a medium sized limiter tokamak with $R_0 = 1.75$ m and a minor radius $a = 0.46$ m. The CR system at TEXTOR [17] consists of two heterodyne reflectometers in the frequency range $24 \leq f_{\text{ref}} \leq 40$ GHz. Both systems are hopping reflectometers with a response time for a change in frequency of $\Delta t \leq 1$ ms and $\Delta t \leq 50$ ms, respectively. The antennae set up consists of three arrays; one at the top and one at the midplane each with five antennae, toroidally separated by $\Delta\phi = 22.5^\circ$, both installed for O-mode operation. A third array at the midplane with three antennae is separated by $\Delta\phi = 112.5^\circ$ and $\Delta\phi \approx 90^\circ$ from the two other arrays, respectively. The antennae set up in the arrays with five antennae, spanning a poloidal angle of 0.1 rad allows, in addition to the measurement of Ω_\perp , the estimation of L_\perp , L_r and τ_{dc} . The estimation of the L_r from reflectometry signals can be hampered by a small angle scattering effect, which results in an overestimation of the turbulence L_r . Therefore it is necessary to characterize the regime in which the measurements are performed in terms of turbulence level ($\delta n/n_c$) and density scale length L_n [2]. Furthermore, as outlined in [18] the contribution of drift waves in two-dimensional linear theory increases the measured L_r , as it is deduced from reflectometry. However, for increasing poloidal wave number (k_θ) of the turbulence the effect decreases nonlinearly. At TEXTOR $k_\perp \approx k_\theta$ is measured together with the radial correlation, allowing us to validate the L_r estimation.

The estimation of the inclination angle α of the turbulent structure from four toroidally and poloidally separated antennae is given by

$$\tan \alpha = \frac{r_c \cdot \Delta\theta(1 - k)}{d(k + 1)}, \quad (2)$$

where the ratio of delay times for two different antennae combinations is given by $k = \Delta t_1 / \Delta t_2$, $d = R_c \delta\phi$ denotes the toroidal distance between the antennae spots on r_c and $\Delta\theta$ is the poloidal distance between the antennae in the array under consideration. As a consequence the projection on v_\perp is different for antennae combination with the same poloidal and toroidal spacing. The relation between the inclination angle and the magnetic pitch angle becomes obvious when reversing the toroidal magnetic field which changes the sign of α [17].

Radial correlation can be determined either for the top position or for the midplane position, by connecting one receiving antennae to the 2nd reflectometer and sharing launching antennae for the 1st and 2nd reflectometers. For LRCs the 2nd midplane antennae array is used either in combination with the top or with the 1st midplane array. In the case of LRC between top and midplane, the O-mode operation and toroidal symmetry of n_e ensures a measurement just at the same r_c . Tailoring the plasma parameter it is possible to study even LRC along a magnetic field line.

5. Recent TEXTOR results

This section describes some recent results obtained from the CR system at TEXTOR. In O-mode the density- and velocity oscillations of GAMs are examined at different poloidal and toroidal positions. In addition, the radial correlation of the ambient turbulence is measured.

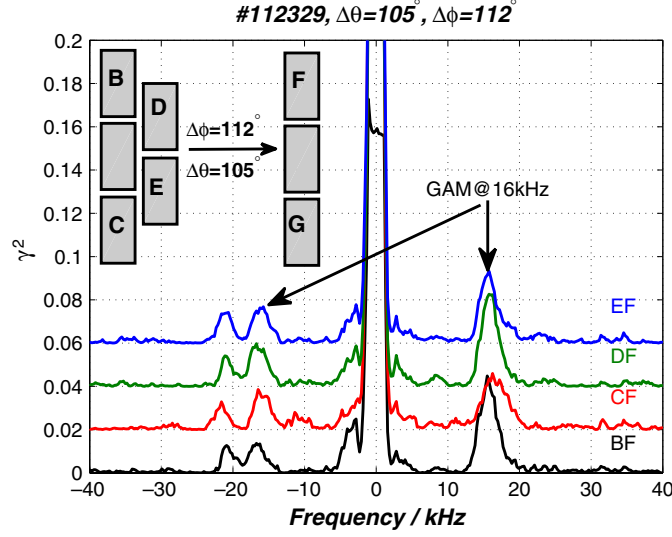


Figure 3. LRC for different antennae combinations, showing a GAM at 16 kHz. Letters denote the different antenna. To distinguish γ^2 for different antennae combinations an offset of 0.02 is added.

5.1. LRC of GAMs and radial structure

At TEXTOR the mode structure of GAMs is best investigated by cross correlations between the top and one midplane array. To demonstrate the long range character of the GAMs the magnitude squared coherence (γ^2) between each antennae of the top array and one antennae of one midplane array is shown in figure 3. The inset in the upper left corner shows the antennae mouth of the two arrays separated poloidally by $\Delta\theta = 105^\circ$ and toroidally by $\Delta\phi = 112^\circ$ with respect to the top array. The single antennae are denoted by capital letters. Due to ensemble averaging ($N_{av} = 100$ ensembles each with 4 ms) a high contrast with respect to the background is found for $f_{GAM} = 16$ kHz at $r/a = 0.81$ for all combinations. It demonstrates the power of the cross-correlation method. The combination with radial correlation gives also insight into the spatial structure of the GAMs. Therefore, the antennae from the midplane array F,G and antennae C from the top array are connected to the hopping reflectometer. The other antennae of the top array (B,D,E) are supplied by the reflectometer operating at constant frequency. To be sure that frequencies of the reflectometer coincide, the coherence spectrum is integrated for the antennae pair with the largest poloidal distance in the top array ($\int \gamma_{BC}^2$). In figure 4 these data are presented by \square symbols. The data can be approached by a Gaussian and the shift of the center of the Gaussian is determined to $\Delta r = 0$ mm, confirming that the frequency of both reflectometers coincides. In addition, the radial LRC is calculated for the complex amplitude and the maximum in magnitude squared coherence ($\max(\gamma_{GAM}^2)$) is shown as a function of Δr for $f_{GAM} = 16$ kHz. A significant shift of the maximum is found (see figure 4, \circ symbols). The positive shift of $\delta r \approx 6$ mm indicates a radial displacement of the GAM at the two toroidally and poloidally separated positions. At the midplane antennae the GAM is more inward than at the top array. The $1/e$ level of the Gaussian yields $L_{GAM} = 11$ mm. It suggests that the GAM has a radial eigenmode [19].

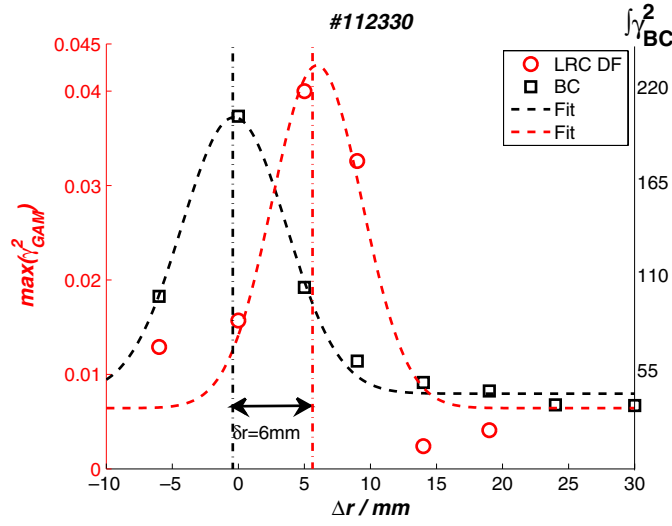


Figure 4. Integrated γ^2 for an antennae pair of the top array (\square) and maximum in γ^2 for $f_{\text{GAM}} = 16$ kHz (\circ). The displacement of the maximum for the GAM denotes a radial outward propagation.

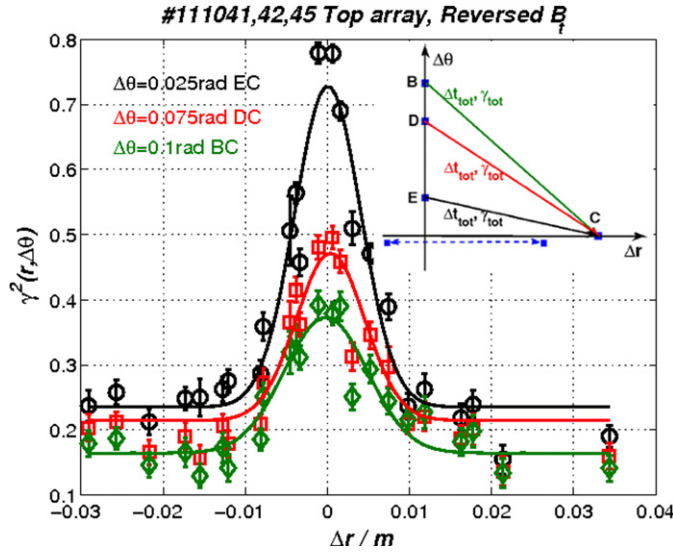


Figure 5. Measurement of the cross-correlation for three different poloidal separations. Each curve is constructed from three discharges with reference frequencies $f = f_0 - 2, f_0, f_0 + 2$ GHz. The \circ symbols denote $\theta = 0.025$ rad; \square symbols denote $\theta = 0.075$ rad and \diamond symbols denote $\theta = 0.1$ rad.

5.2. Radial correlations

The system at TEXTOR measures always a combination of poloidal and radial correlations if both systems operate at different frequencies. Supplying only one antennae (C) to sweeping reflectometer and operating all other antennae at a fixed frequency, each combination with antennae C has in addition to the radial a poloidal component (see inlet of figure 5). $L_r(\theta)$ is measured in ohmic plasmas with $350 \leq I_p \leq 400$ kA, $1.9 \leq B_t \leq 2.25$ T and a line

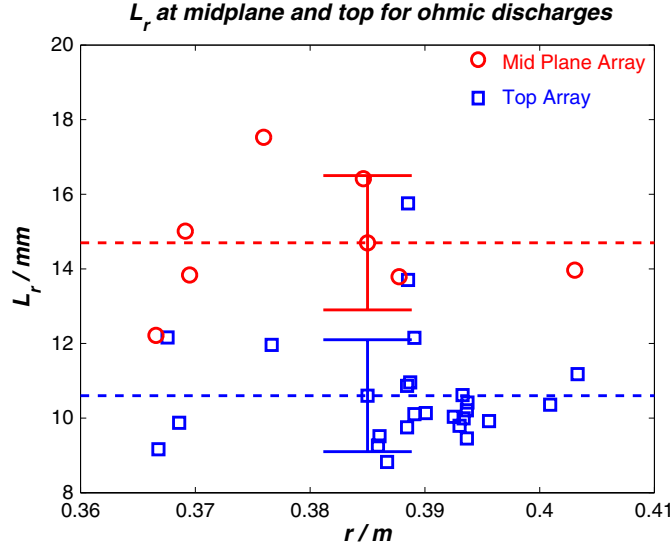


Figure 6. L_r for top and midplane array. The dashed line denotes the mean values obtained from the top and midplane array, respectively.

averaged electron density of $2e19 \leq \bar{n}_e \leq 2.5e19 \text{ m}^{-3}$. The measurements are performed in the range $0.78 \leq r/a \leq 0.89$. For each discharge, eight different radial positions are probed. Measuring $\gamma^2(\Delta r)$, where Δr is the radial separation between the two reflection layers, a Gaussian distribution is obtained for every $\Delta\theta$ (see figure 5). With increasing $\Delta\theta$ the amplitude of the Gaussian decreases and the measured full width at $1/e$ level, corresponding to $L_r(\theta)$ is slightly increasing. Extrapolating $L_r(\Delta\theta)$ toward $\Delta\theta = 0$ provides L_r from the reflectometry signals. Following the discussion in [2, 18] in the linear regime (low turbulence level $\delta n/n_c$) and for the typical high poloidal wave number ($k_\perp \approx 300 \text{ m}^{-1}$) and small density scale length ($L_n \approx 0.1 \text{ m}$) the measured correlation length matches the radial correlation length of the turbulence. This is also confirmed by the fast decay of γ^2 for small normalized cut off separations [18].

The CR system at TEXTOR can be operated with the top and the equatorial antennae array. With the two poloidal arrays the scaling of L_r with the local ion gyration radius ρ_i is proved. The results are shown in figure 6 where the top array yields always smaller L_r compared with the midplane array. The dashed lines denote the mean value which is estimated for the top array $L_r = 10.6 \pm 1.5 \text{ mm}$ and $L_r = 14.7 \pm 1.8 \text{ mm}$ is obtained for the midplane array. With O-mode CR the measurement at the top and midplane is performed at the same flux surface. For normalized ion gyration radius $\rho^* = \rho_i/a$, a key property in the characterization of the turbulence, the $1/r$ dependence of B_t determines the turbulence radial correlation length. It confirms that the correlation length obeys a gyro-Bohm-like scaling. The scaling with ρ_i yields: $5 \leq L_r/\rho_i \leq 6$, where ρ_i is calculated for $T_e = T_i$. Similar results are obtained at DIII-D [20] yielding $L_r \approx 5\rho_i$ at the midplane for low- and high-confinement plasmas.

6. Summary

CR is a mighty tool for the investigation of plasma turbulence and its propagation. Under the assumption that the turbulence is nearly frozen in the plasmas the perpendicular plasma rotation

can be measured. Whereas the standard CR systems are restricted to low k_{\perp} correlation, Doppler reflectometry can extend this range to higher k_{\perp} . In particular, the simultaneous measurement of $\delta n/n_c$ and δv makes CR a powerful diagnostic. Using O-mode propagation and antennae arrays at different poloidal and/or toroidal positions allows us to probe the plasma per definition at the same isodensity layer. This makes the measurement of LRC more easy. CR systems are installed at several devices and used for the measurement of Ω_{\perp} , L_{\perp} , L_r and τ_{dc} . Estimation of L_r may be affected by small angle scattering and the level of $\delta n/n_c$. Toroidally and poloidally slightly displaced antennae can provide information on the inclination angle of turbulent structures, which can be used for the measurement of the local safety factor.

At TEXTOR the LRC properties of the GAM are measured. The measurement of L_r is performed in ohmic plasmas at TEXTOR and confirms the gyro-Bohm-like scaling of L_r from measurements at top and midplane.

Euratom © 2011.

References

- [1] Nazikian R, Kramer G J and Valeo E 2001 *Phys. Plasmas* **8** 1840–55
- [2] Gusakov E Z and Popov A Yu 2002 *Plasma Phys. Control. Fusion* **44** 2327–37
- [3] Davidson P A 2004 *Turbulence* (Oxford: Oxford University Press)
- [4] Conway G, Schirmer J, Kluge S, Suttrop W and Holzhauser E 2004 *Plasma Phys. Control. Fusion* **46** 951–70
- [5] Krämer-Flecken A, Soldatov S, Busch C, Liang Y, von Hellermann M and Wolf R 2006 *Nucl. Fusion* **46** S730–42
- [6] Stepanov A Yu *et al* 1997 *Fusion Eng. Des.* **34–35** 507–10
- [7] Gilmore M, Peebles W A and Nguyen X V 2001 *Rev. Sci. Instrum.* **72** 293
- [8] Vershkov V A *et al* 2001 *28th EPS Conf. on Controlled Fusion and Plasma Physics (Funchal, Madeira)* vol 25A, pp 65–8
- [9] Vershkov V A *et al* 2005 *Nucl. Fusion* **45** S203–26
- [10] Vershkov V A *et al* 2010 *23rd IAEA Fusion Energy Conf. (Daejeon, Korea, 11–16 October 2010)*
- [11] Conway G, Vayakis G, Fessey J A and Barlett D V 1999 *Rev. Sci. Instrum.* **70** 3921
- [12] Hacquin S, Meneses L, Cupido L, Cruz N, Kokonchev L, Prentice R and Gowers C 2004 *Rev. Sci. Instrum.* **75** 3834
- [13] Figueiredo A C A, Fonseca A and Meneses L 2008 *Rev. Sci. Instrum.* **79** 10F107
- [14] Hirsch M and Holzhauser E 2004 *Plasma Phys. Control. Fusion* **46** 593–609
- [15] Schirmer J, Conway G D, Holzhauser E, Suttrop W and Zohm H 2007 *Plasma Phys. Control. Fusion* **49** 1019–39
- [16] Hennequin P, Honoré C, Truc A, Quéméneur A and Lemoine N 2004 *Rev. Sci. Instrum.* **75** 3881
- [17] Krämer-Flecken A, Soldatov S, Vowinkel B and Müller P 2010 *Rev. Sci. Instrum.* **81** 113502
- [18] Gusakov E Z and Yakovlev B O 2002 *Plasma Phys. Control. Fusion* **44** 2525–37
- [19] Itoh S, Itoh K, Sasaki M, Fujisawa A, Ido T and Nagashima Y 2007 *Plasma Phys. Control. Fusion* **49** L7–L10
- [20] McKee G R *et al* 2001 *Nucl. Fusion* **41** 1235–42